Human Immunodeficiency Virus Type 1 Vpr-Binding Protein VprBP, a WD40 Protein Associated with the DDB1-CUL4 E3 Ubiquitin Ligase, Is Essential for DNA Replication and Embryonic Development[▽]

Chad M. McCall,[1,2]‡ Paula L. Miliani de Marval,[1,2]‡ Paul D. Chastain II,[3] Sarah C. Jackson,[1,2] Yizhou J. He,[1,2] Yojiro Kotake,[1,2] Jeanette Gowen Cook,[1,2] and Yue Xiong[1,2,4]*

Department of Biochemistry and Biophysics,[1] Lineberger Comprehensive Cancer Center,[2] Department of Pathology and Laboratory Medicine,[3] and Program in Molecular Biology and Biotechnology,[4] University of North Carolina School of Medicine, Chapel Hill, North Carolina 27599

Damaged DNA binding protein 1, DDB1, bridges an estimated 90 or more WD40 repeats (DDB1-binding WD40, or DWD proteins) to the CUL4-ROC1 catalytic core to constitute a potentially large number of E3 ligase complexes. Among these DWD proteins is the human immunodeficiency virus type 1 (HIV-1) Vpr-binding protein VprBP, whose cellular function has yet to be characterized but has recently been found to mediate Vpr-induced G_2 cell cycle arrest. We demonstrate here that VprBP binds stoichiometrically with DDB1 through its WD40 domain and through DDB1 to CUL4A, subunits of the COP9/signalsome, and DDA1. The steady-state level of VprBP remains constant during interphase and decreases during mitosis. VprBP binds to chromatin in a DDB1-independent and cell cycle-dependent manner, increasing from early S through G_2 before decreasing to undetectable levels in mitotic and G_1 cells. Silencing *VprBP* reduced the rate of DNA replication, blocked cells from progressing through the S phase, and inhibited proliferation. *VprBP* ablation in mice results in early embryonic lethality. Conditional deletion of the *VprBP* gene in mouse embryonic fibroblasts results in severely defective progression through S phase and subsequent apoptosis. Our studies identify a previously unknown function of VprBP in S-phase progression and suggest the possibility that HIV-1 Vpr may divert an ongoing chromosomal replication activity to facilitate viral replication.

Ubiquitin ligases play a critical role in cellular function by recruiting various protein substrates for covalent modification by the small protein ubiquitin (15, 31). Ubiquitin modification, either monomeric or in polyubiquitin chains, leads to various changes in cellular protein function, most prominently the targeting of polyubiquitin-conjugated proteins to the 26S proteasome for proteolytic degradation. The cullin family of ubiquitin ligases performs remarkably broad functions due to their ability to assemble a large number of distinct cullin-RING E3 ligase complexes through modular interaction with substrate receptors containing specific protein-protein interaction motifs (29). Cullins interact with their substrate receptors either directly, as in the case of CUL3, which interacts with one of more than 200 BTB domain-containing receptors (10, 11, 32, 43), or indirectly through a conserved linker protein, such as the SKP1 protein that bridges one of more than 70 F-box-containing receptors to CUL1 (2, 9, 36) and the heterodimer of elongins B and C that links one of the more than 30 VHL-box or SOCS-box receptors with CUL2 or CUL5 (21, 22, 38, 44). Through interaction with these common motifs, the cullin-RING E3 ligase complexes may potentially ubiquitinate a large number of substrates.

We along with other groups recently discovered that *dam*-aged *D*NA *b*inding protein 1, DDB1, acts a linker protein for CUL4 and recruits substrates through interaction with a subset of WD40 proteins (1, 14, 16, 19). Mammalian cells contain at least 90 *D*DB1-binding *WD*40 (DWD) proteins (also known as DCAF for *D*db1- and *C*ul4-*a*ssociated *f*actors and CDW for *C*UL4 and *D*DB1-associated *WD*40 repeats), suggesting that CUL4-ROC1 ligases may also promote ubiquitination of a large number of substrates. One of the more than 30 mammalian DWD proteins that have been experimentally demonstrated to bind DDB1-CUL4 is VprBP/DCAF1 (accession number NM014703), a 170-kDa protein that was initially identified through coimmunoprecipitation and peptide sequencing of HIV-1 Vpr-binding proteins (VprBPs) (45). Very recently, it has been shown that VprBP is required for the G_2 cell cycle arrest caused by Vpr expression (3, 8, 17, 24, 35, 39, 42). The physiological significance underlying the Vpr-VprBP interaction for human immunodeficiency virus (HIV) viral propagation remains unclear. VprBP orthologs are found in *Drosophila melanogaster* (36% identical to human VprBP), *Caenorhabditis elegans* (31%), and *Arabidopsis thaliana* (27%), but no obvious ortholog is recognizable in yeast cells. VprBP is broadly expressed in most, if not all, human and mouse tissues that have been examined (45). These features suggest an unknown but conserved and possibly critical function of VprBP in multicellular organisms. This study is directed toward elucidating this issue.

MATERIALS AND METHODS

Antibodies, immunopurification, and mass spectrometric analysis. Antibodies to hemagglutinin ([HA] 12CA5; Boehringer-Mannheim), Myc (9E10; NeoMarkers),

* Corresponding author. Mailing address: 22-012 Lineberger Cancer Center, University of North Carolina at Chapel Hill, Chapel Hill, NC 27516-7295. Phone: (919) 962-2142. Fax: (919) 966-8799. E-mail: yxiong@email.unc.edu.
‡ These authors contributed equally to this work.
▽ Published ahead of print on 7 July 2008.

T7 (Novagen), FLAG (M2; Sigma), p53 (DO-1; NeoMarkers), p21 (NeoMarkers), histone H3 (Abcam), alpha-tubulin (NeoMarkers), MCM2 (B58720; Transduction Laboratories), ORC2 (559266; BD Pharmagen), and CSN5 (JAB1; GeneTex) were purchased commercially. Rabbit polyclonal antibodies to CUL4A, DDB1, and CDT1 have been described previously (18). A rabbit polyclonal antibody against VprBP was produced by injection of a synthetic peptide antigen into residues 1493 to 1507 of VprBP (DNSDLEDDIILSLNE). To purify the endogenous CUL4A complex, BT474 cells from 47 150-mm plates were lysed with a 0.5% NP-40 lysis buffer (50 mM Tris-HCl at pH 7.5, 150 mM NaCl, 0.5% NaCl, 50 mM NaF), and lysates were pooled (300 mg total). Clarified lysates were immunoprecipitated with affinity-purified anti-CUL4A antibody (2 µg/mg lysate with or without 10 µg/mg antigen peptide). Immunocomplexes were resolved by sodium dodecyl sulfate-polyacrylamide gel electrophoresis (SDS-PAGE) and stained with Coomassie blue, and the protein bands were digested with trypsin and subjected to mass spectrometric analysis at the University of North Carolina Proteomics Core Facility. To purify the endogenous VprBP complex, an analogous protocol was used but with U2OS cells.

Plasmids, cell culture, and cell transfection. Plasmids expressing human CUL4A and DDB1 were as previously described (14, 18). pFSZ2-VprBP-FLAG was the kind gift of L. J. Zhao (St. Louis University) and was used to subclone VprBP into a pcDNA3-based mammalian expression vector. Mutations were introduced by site-directed mutagenesis using a QuikChange kit (Stratagene) and verified by DNA sequencing. Cell lines were cultured as follows: HeLa cells were cultured in Dulbecco's modified Eagle's medium containing 10% fetal bovine serum (FBS) in a 37°C incubator with 5% CO_2; U2OS cells were cultured in McCoy's 5A medium containing 15% FBS; HCT116 cells were cultured in McCoy's 5A medium containing 10% FBS; WI-38 and WI-38/E6 cells were cultured in minimal essential medium with sodium pyruvate, nonessential amino acids, and 10% FBS; and 293T cells were cultured in Dulbecco's modified Eagle's medium containing 10% newborn calf serum. Cell transfections were carried out using a calcium-phosphate buffer.

Gel filtration chromatography. To examine the elution profile of CUL4A and associated proteins, HeLa cells were lysed with the 0.5% NP-40 lysis buffer, and clarified lysate was resolved through a Superdex 200 gel filtration column (GE/Amersham). Fractions (0.5 ml) were collected, and 50 µl of each was resolved via SDS-PAGE and immunoblotted with antibodies as indicated on the figures. High-molecular-weight standards (GE/Amersham) were resolved through the same column, and the peak fraction for each was determined.

RNA interference. Recombinant Dicer-generated small interfering RNA (siRNA) to VprBP was generated by first amplifying bp 4008 to 4625 of VprBP cDNA using PCR primers with 5′ overhangs with T7 promoter sequences. This PCR product was then used as a template for in vitro transcription of both strands of a double-stranded RNA (dsRNA) by using a T7 RiboProbe kit (Promega) and then annealing the dsRNA by heating the transcribed mixture to 95°C and slowly cooling it to room temperature. This dsRNA was then immediately added, without purification, to a reaction mixture containing 8 U of recombinant Dicer (Stratagene) and Dicer reaction buffer to a total of 500 ml. After being digested for 18 h at 37°C, the Dicer products were purified by a series of three spin columns (G-25 [Amersham, Piscataway, NJ], EZ-pure [Millipore, Bedford, MA], and Microcon-100 [Millipore]) (27). The final product was resolved on a 15% native polyacrylamide gel along with a known quantity of a synthetic siRNA to estimate the final concentration. Control green fluorescent protein-recombinant Dicer siRNAs were prepared as described previously (27).

Two duplex oligonucleotides encoding human VprBP-specific short hairpin RNA (shRNA) (sh1, 5′-CCGGGAATACTCTTCAAGAATGATGCCTCCTG TCACATCATTCTTGAAGAGTATTCTTTTTG-3′; sh2, 5′-CCGGGAAATA CCTCGTCCTTCTATGCTTCCTGTCACATAGAAGGACGAGGTATTTCT TTTTG), one duplex encoding human DDB1-specific shRNA (5′-CCGGCAG CATTGACTTACCAGGCATCCTCCTGTCAATGCCTGGTAAGTCAATGC TGTTTTTG-3′), and one duplex oligonucleotide encoding firefly luciferase-specific shRNA (5′-CCGGGAGCTGTTTCTGAGGAGCCCCTCCTGTCAGGCT CCTCAGAAACAGCTCCCGGTTTTTG-3′) were ligated into the pMKO.1 vector (Addgene plasmid 8452). Retrovirus production and transduction were carried out according to a standard protocol. Twenty-four hours after infection, noninfected cells were removed by the addition of puromycin (2 µg/ml) for 2 days before analysis for cell cycle, cell proliferation, protein expression, and complex formation. The siRNA sequence targeting DDB1 used in the experiment shown in Fig. 5C was previously described (35) and was transfected to HCT116 cells using Dharmafect (Dharmacon).

Flow cytometry. To analyze DNA content by propidium iodide (PI) staining, cells were fixed in 75% ethanol overnight at 4°C, washed once in 1× phosphate-buffered saline (PBS) plus 1% FBS, and then permeabilized for 30 to 45 min at 37°C in 1× PBS, 0.1 mg/ml RNase A, and 0.1% Triton X-100. The fixed and permeable cells were stained with 50 µg/ml PI for at least 90 min at room temperature, shielded from light. To analyze ongoing replication of DNA by bromodeoxyuridine (BrdU) labeling, cells were fixed in 80% ethanol overnight at 4°C and then washed once in 1× PBS. Nuclei were isolated by incubating cells in 0.1 M HCl–0.08% pepsin for 20 min at 37°C, and then DNA was denatured by incubating cells in 2 M HCl for a further 20 min at 37°C. After the HCl was neutralized with 2 volumes of 0.1 M sodium borate, pH 8.5, the cells were washed once with immunofluorescence assay (IFA) buffer (10 mM HEPES [pH 7.3], 150 mM NaCl, 4% FBS, 0.1% sodium azide) plus 0.5% Tween 20. The cells were labeled with fluorescein isothiocyanate (FITC)-conjugated anti-BrdU (BD Biosciences) at 1:10 in IFA buffer plus Tween for 45 min at room temperature and then washed once with IFA buffer plus Tween. Finally, cells were stained for DNA content by incubation for 30 min at room temperature with IFA buffer–0.1 mg/ml RNase A–50 mg/ml PI. Stained cells were analyzed at the University of North Carolina School of Medicine Flow Cytometry Facility on either a FACScan (Becton Dickinson) or CyAN (Dako Cytomation) flow cytometer, and data were analyzed using Summit software, version 4.3 (Dako Cytomation).

Molecular combing. To analyze the properties of replication forks, HeLa cells were double labeled by incubation, first in medium with 100 µM iododeoxyuridine (IdU) for 10 min and second in 50 µM chlorodeoxyuridine (CldU) for 20 min. DNA spreads were generated and stained for IdU and CldU, and individual replication tracks were analyzed as described previously (41).

Chromatin fractionations. Cells were lysed in CSK buffer (10 mM PIPES-KOH [pH 6.8], 100 mM NaCl, 300 mM sucrose, 3 mM $MgCl_2$, 0.5 mM phenyl-methylsulfonyl fluoride, 1 mM glycerophosphate, 50 mM NaF, 1 mM Na_3VO_4, and protease inhibitor cocktail tablet) containing 0.5% Triton X-100 as described in Cook et al. (7). Portions were reserved (whole-cell extracts) prior to fractionation by low-speed centrifugation. Detergent-insoluble pellets were treated for 5 min with 15 U of micrococcal nuclease (Roche) in CSK buffer supplemented with 2 mM $CaCl_2$ and then separated again by centrifugation. Proteins in the nuclease-soluble fractions of these digests were defined as chromatin bound. Densitometry analysis was performed using the public domain NIH Image program (U.S. National Institutes of Health [http://rsb.info.nih.gov/nih-image/]).

Generation of VprBP mutant mice and mouse embryonic fibroblasts (MEFs). A 9.3-kb fragment of mouse genomic DNA, spanning from exon 5 to intron 8 of the *VprBP* gene, was amplified by PCR from mouse 129 SvEv embryonic stem (ES) cell genomic DNA and verified by DNA sequencing. LoxP sites were inserted at the 5′ and 3′ ends of a 2,358-bp genomic fragment containing exons 7 and 8 encoding 203 amino acid residues (Val172 to Ala374). To select for homologous recombination, a neomycin resistant gene (Neo^r), flanked by Flp recognition target sites, was inserted immediately upstream of the 5′ LoxP deletion site, and a thymidine kinase negative selection marker was inserted upstream of exon 5. Following homologous recombination into ES cells, Cre or Flp recombinase expression vectors were transiently transfected to delete either the targeted exons (exon 7 and 8) or the Neo^r cassette. The recombination event was confirmed by Southern blot analysis with probes against either exons 5 and 6 (probe 2) or exons 7 and 8 (probe 1). Three independent clones were injected into C57BL/6 blastocysts, and the resulting chimeras were mated with C57BL/6 females to generate VprBP^floxΔ/+ or VprBP^Δfrt/+ heterozygous mice. Transmission of the targeted loci was confirmed by Southern blotting and PCR. Heterozygous offspring were intercrossed to produce homozygous mutant animals. Primers for genotyping the conventional knockout mice were the following: FW-5′-TGAGTGGTTGGATCCGTACTAC-3′, RV-5′-TTAAGGCCTGTCGA CAAGCG-3′, and RV-5′-CCCAAACTAGAAGGTGTGCA-3′. Primers for genotyping the conditional mice were FW-5′-GCATACATTATACGAAGTTATGG ATCC-3′ and RV-5′-GTATGCTATACGAAGTTATGCTAGCCT-3′.

To generate the VprBP null MEFs, we mated heterozygous VprBP^floxΔ/+ and VprBP^Δfrt/+ mice. Embryos were isolated at day 13.5 post coitus (E13.5). MEFs at early passages were infected with empty vector (pMX) or pMX-Cre recombinase expressing retrovirus (kindly provided by Keiichi Nakayama). Two days after infection MEFs were selected with 2 µg/ml of puromycin for 2, 4, or 10 days before cell cycle analysis.

RESULTS

VprBP associates with DDB1-CUL4 E3 ligase complex. We previously used large-scale immunoprecipitation and mass spectrometry to identify a series of CUL4A/DDB1-interacting proteins and used this approach to define a common motif found in potential CUL4A/DDB1 substrate receptors, the DWD box (14). The most abundant of these DWD proteins in
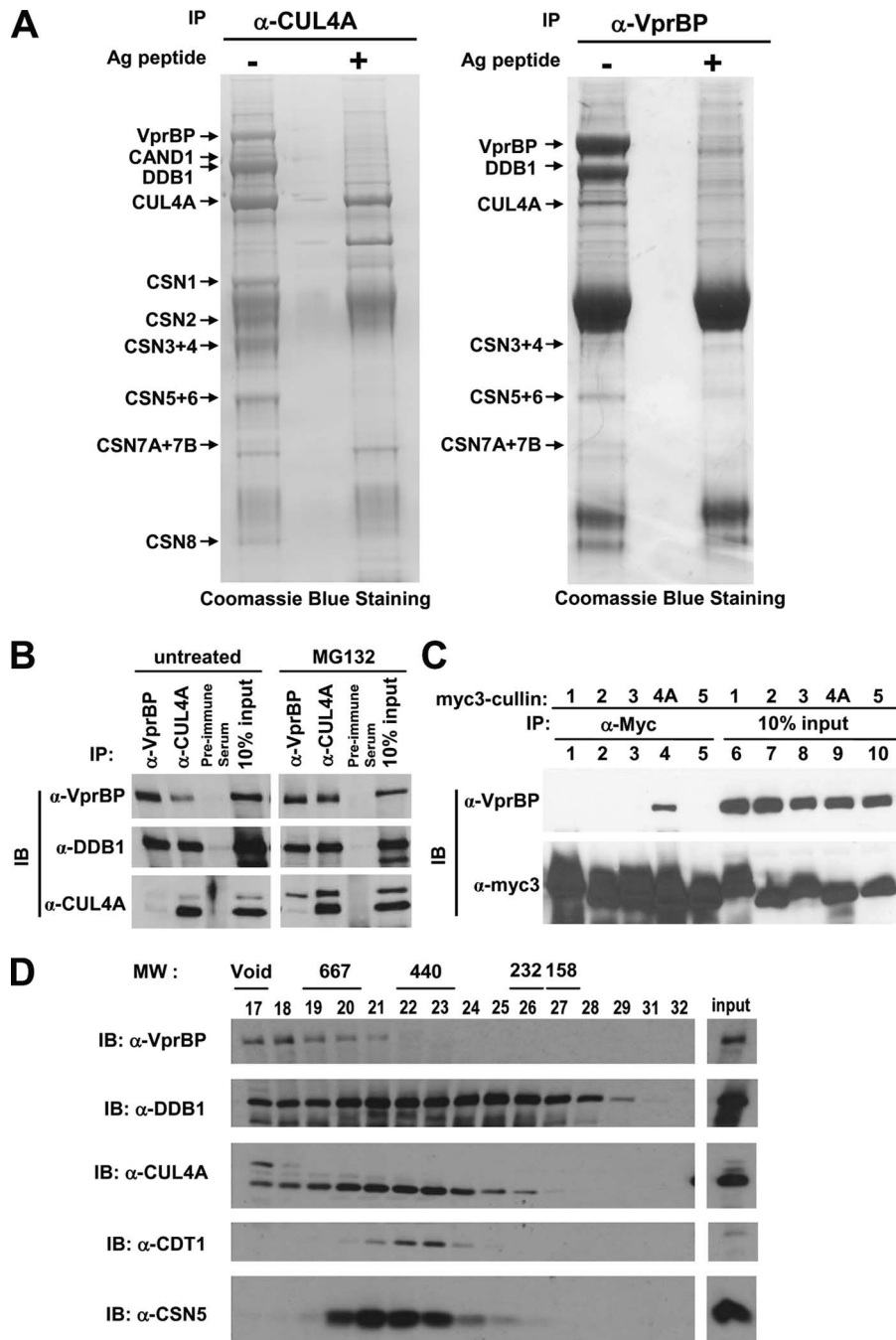
FIG. 1. VprBP specifically associates with DDB1-CUL4 E3 ligase. (A) CUL4A and VprBP complexes were immunopurified from human BT474 cells and U2OS cells, respectively, and resolved by SDS-PAGE, followed by staining with Coomassie brilliant blue. Bands identified by mass spectrometry are indicated. Subunits of the COP9/signalosome (CSN) are indicated. (B) Endogenous VprBP and CUL4A coimmunoprecipitate. U2OS cells were treated with MG132 (25 μM for 5 h) and then lysed with 0.5% NP-40 lysis buffer and immunoprecipitated with antibodies against VprBP or CUL4A. Immunocomplexes were resolved by SDS-PAGE and immunoblotted with the indicated antibodies. Proteins identified by mass spectrometry are indicated with arrows. (C) VprBP associates with CUL4A but not other cullins. 293T cells were transfected with pcDNA3-myc3-cullin plasmids, and lysates were immunoprecipitated and immunoblotted as indicated. (D) VprBP exists in very-high-molecular-weight complexes. An NP-40 lysate derived from HeLa S3 cells was resolved on a Superdex 200 gel filtration column, along with molecular weight standards as indicated. The void volume corresponded to a molecular mass over 700 kDa, and the input control was 100 μg of HeLa S3 lysate. Equal volumes of each fraction were resolved by SDS-PAGE and immunoblotted as indicated. IP, immunoprecipitation; IB, immunoblotting; α, anti; Ag, antigen; MW, molecular weight (in thousands).

our CUL4A immunocomplex was VprBP(Fig. 1A, left panel). To characterize VprBP, we generated a rabbit polyclonal antibody to VprBP, performed a large-scale immunoprecipitation in U2OS cells (Fig. 1A, right panel), and submitted bands

that were specifically competed off by antigen peptide for mass spectrometric identification. We found, as determined by Coomassie blue staining, that VprBP associated with almost stoichiometric amounts of DDB1, smaller amounts of CUL4A, the

subunits of the COP9/signalosome deneddylase, and DDA1 (for DDB1-associated 1; also called DET1) (30). In order to verify the specificity of these interactions, we performed immunoprecipitation and immunoblotting experiments (Fig. 1B). VprBP coimmunoprecipitated preferentially with NEDD8-modified CUL4A, which was more noticeable upon enrichment of CUL4A-NEDD8 by proteasome inhibition. Since both binding with COP9/signalsome subunits and neddylation of CUL4 are associated with active cullin ligases, it is likely that VprBP is associated with the active form of DDB1-CUL4-ROC1.

To determine if VprBP specifically binds CUL4-DDB1 or if it binds all cullin family members, we immunoprecipitated ectopically expressed individual cullins and performed immunoblotting assays for endogenous VprBP (Fig. 1C). VprBP was detected only in the CUL4A immunocomplex and not in any of four other cullins we examined, suggesting that VprBP functions specifically through CUL4.

The Coomassie blue-stained immunocomplex suggested that VprBP might interact with multiple cellular proteins. To test this idea specifically, we separated a lysate of HeLa cells by gel filtration chromatography (Fig. 1D). VprBP exists in complexes of more than 450 kDa to greater than 700 kDa in size, and we were unable to detect by Western blotting any VprBP in size fractions corresponding to a monomeric form. This finding, combined with the presence of abundant DDB1 in the VprBP immunocomplex, implies that VprBP primarily functions through its interactions with the CUL4A ubiquitin ligase as opposed to acting as a monomer. All of the fractions that contained VprBP also contained abundant DDB1 and CUL4. These results suggest that DDB1 is a major functional partner of VprBP in vivo and that VprBP, through DDB1, associates with CUL4-based E3 ligase complexes.

The WD40 domain of VprBP and the N-terminal domain of CUL4A are both required and sufficient for binding of VprBP with DDB1-CUL4A. We have previously shown that the N terminus of CUL4A interacts with DDB1 and that DDB1 functions as a linker to recruit DWD proteins (14, 18). To verify that VprBP is likewise recruited to the CUL4 complex, we coexpressed VprBP with a panel of CUL4A mutants (Fig. 2A) and found that deletion of the N-terminal 52 or 100 amino acids, which constitute the DDB1-interaction domain, completely abrogated the VprBP-CUL4A interaction (Fig. 2B), providing further support that DDB1 bridges VprBP to CUL4A. In addition to its C-terminal WD40 domain, VprBP contains conserved domains in its N terminus. We examined whether these domains might influence its binding to CUL4A/DDB1. Expression of the C terminus of VprBP alone, containing the WD repeats and a highly acidic "tail," was sufficient to bind endogenous CUL4A and DDB1, indeed, even more abundantly than full-length VprBP (Fig. 2C). This observation, combined with the inability of the conserved N-terminal domain (N-terminal 751 residues of VprBP) to interact with CUL4A or DDB1, indicates that VprBP interacts with DDB1-CUL4 through its WD40 domain.

VprBP expression is essential for normal proliferation and DNA replication. To explore the cellular function of VprBP through the use of RNA interference, we first used recombinant Dicer to generate siRNA to VprBP (Fig. 3A). Efficient VprBP silencing was achieved, resulting in a more than 90% reduction of VprBP protein in transfected U2OS cells (Fig. 3A) and an obvious proliferation defect. To quantify that phenotype, we transfected U2OS cells with siRNA silencing VprBP as well as DDB1 and plated equal numbers of cells 72 h after transfection to measure cellular proliferation. We found that silencing VprBP as well as DDB1 strongly inhibited U2OS cell proliferation (Fig. 3B).

To confirm this result with different siRNA sequences and in different cell lines, we produced three hairpin RNA sequences targeting different regions of VprBP and identified two that were very successful at silencing (Fig. 3C) and at reproducing the siRNA growth arrest phenotype (Fig. 3D). Transduction of a retrovirus expressing one of the two shRNA constructs induced nearly complete silencing (Fig. 3E) and a pronounced S-phase accumulation compared with control luciferase shRNA-infected HeLa cells (Fig. 3F). Treatment of VprBP-silenced cells with the S-phase inhibitor hydroxyurea, thymidine, or aphidicolin (not shown) did not result in further accumulation of S-phase cells (27.9% in untreated cells versus 27.6% in hydroxyurea-treated or 23.8% thymidine-treated cells), whereas the same treatment with luciferase siRNA increased S-phase cells from 12.7% to 35.5% in hydroxyurea-treated and 40.3% in thymidine-treated cells (Fig. 3F). Treatment of VprBP-silenced cells with the metaphase inhibitor nocodazole caused a substantially reduced G_2/M accumulation (from 17% to 25.9%) compared with control luciferase-silenced cells (from 12.7% to 59.9%). Together, these results indicate that silencing of VprBP caused almost complete cessation of DNA synthesis in HeLa cells.

The function of VprBP is required for progression through S phase. To further characterize the S-phase phenotype of cells lacking VprBP, we pulse-labeled HeLa cells with BrdU for 30 min and examined the pattern of its incorporation (Fig. 4A). The percentage of BrdU-positive cells was increased in VprBP-silenced (35%) cells compared with control cells transfected with shRNA targeting luciferase (26%). The rate of BrdU incorporation, however, was markedly reduced in VprBP-silenced cells, with the mean BrdU intensity in VprBP-silenced cells (50 arbitrary units) reduced to slightly less than half that of control cells (96 arbitrary units). To determine whether silencing VprBP had the same or different effects on BrdU incorporation throughout S phase, we gated S-phase cells into six different periods (R1 to R6) and calculated the mean BrdU intensity of each period. Silencing VprBP had very little effect, if any, on the rate of BrdU incorporation in cells in immediate-early S phase, reducing mean BrdU intensity only slightly from 46 in control cells to 44 in VprBP-silenced cells (Fig. 4B, R1 population). Silencing VprBP, however, progressively reduced the mean BrdU intensity in cells progressing through S phase, with cells at middle and later S phase showing the most profound reduction of BrdU incorporation (Fig. 4B). The mean BrdU intensity was reduced from 69 in control cells to 50 in VprBP-silenced cells during early S phase (R2 population), from 93 to 57 and from 126 to 63 for two middle S-phase populations (populations R3 and R4, respectively), from 139 to 60 for a middle-to-late S-phase population (R5), and from 112 to 60 in a late-S-phase population (R6). These results are consistent with a model where VprBP performs a critical function for S-phase progression but not for S-phase entry.
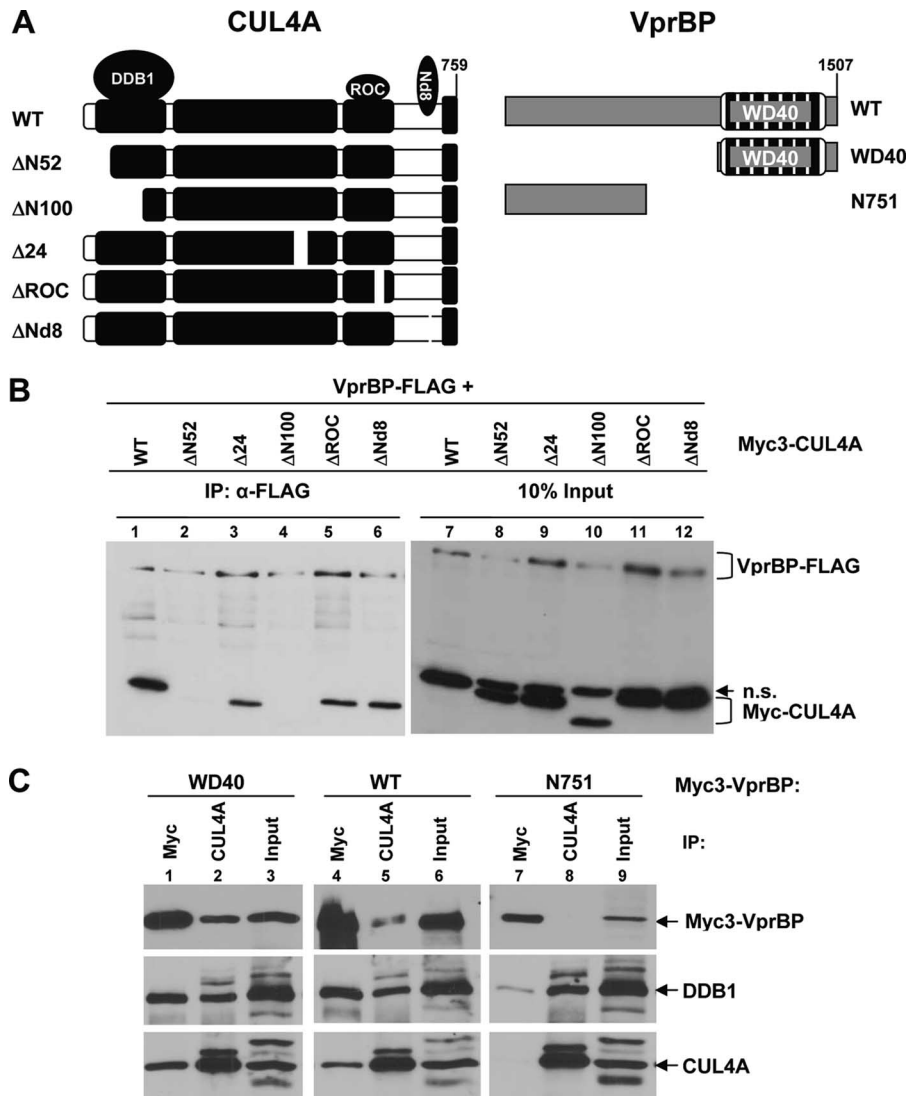
FIG. 2. The WD domain of VprBP is sufficient to interact with CUL4A/DDB1. (A) Schematic diagrams of CUL4A and VprBP mutants used in panels B and C. (B) VprBP interacts with the substrate-recruiting N terminus of CUL4A. 293T cells were transfected with pFSZ2-VprBP-FLAG and pcDNA3-myc3-CUL4A plasmids as indicated. NP-40 (0.5%) lysates were immunoprecipitated with anti-FLAG (M2), resolved by SDS-PAGE, and immunoblotted as shown. The CUL4A mutants used are diagrammed in panel A. (C) The WD domain of VprBP is sufficient to interact with CUL4A/DDB1. 293T cells were transfected with pcDNA3-myc3-VprBP, wild-type, or mutants as indicated. VprBP-DDB1/CUL4 interactions were determined by immunoprecipitation-Western blotting with the indicated antibodies. WT, wild type; IP, immunoprecipitation; n.s., nonspecific; α, anti; N751, conserved N-terminal domain of VprBP; WD40, residues 994 to 1507 of VprBp; ΔN52 and ΔN100, deletion of the N-terminal 52 and 100 residues of CUL4A, respectively; Δ24, deletion of residues 439 to 462; ΔROC, deletion of residues 594 to 612; ΔNd8, K705R mutated Nedd8 conjugation site.

VprBP silencing decreases active replication forks and increases new origin firing. We considered several possibilities to explain the defect in S-phase progression, including defects in replication origin licensing, the ability to activate origins, replication fork elongation, and replication fork stability. To evaluate origin firing and fork elongation, we conducted DNA fiber analysis to examine the replication of DNA at individual replication forks. HeLa cells were transduced with retrovirus expressing shRNA targeting either control luciferase or VprBP. At 72 or 90 h after viral transduction, cells were first labeled for 10 min with IdU and then washed and labeled for 20 min with CldU. After the second pulse, cells

were harvested; a portion was lysed on a glass slide, the slide was tilted, and the DNA fibers were gently straightened and aligned (combed). The DNA fibers were then fixed, and the presence of IdU or CldU was detected by immunostaining with red (AlexaFluor 594) and green (AlexaFluor 488) fluorescent antibodies, respectively. The DNA fiber-labeling technique allowed us to distinguish between replication forks that were active during both the first and second pulses (ongoing forks), forks that initiated only during the second pulse (newly fired origins), and forks that were active only during the IdU pulse (terminations) (Fig. 4C, left panel). The relative proportions of tracks with different label com-
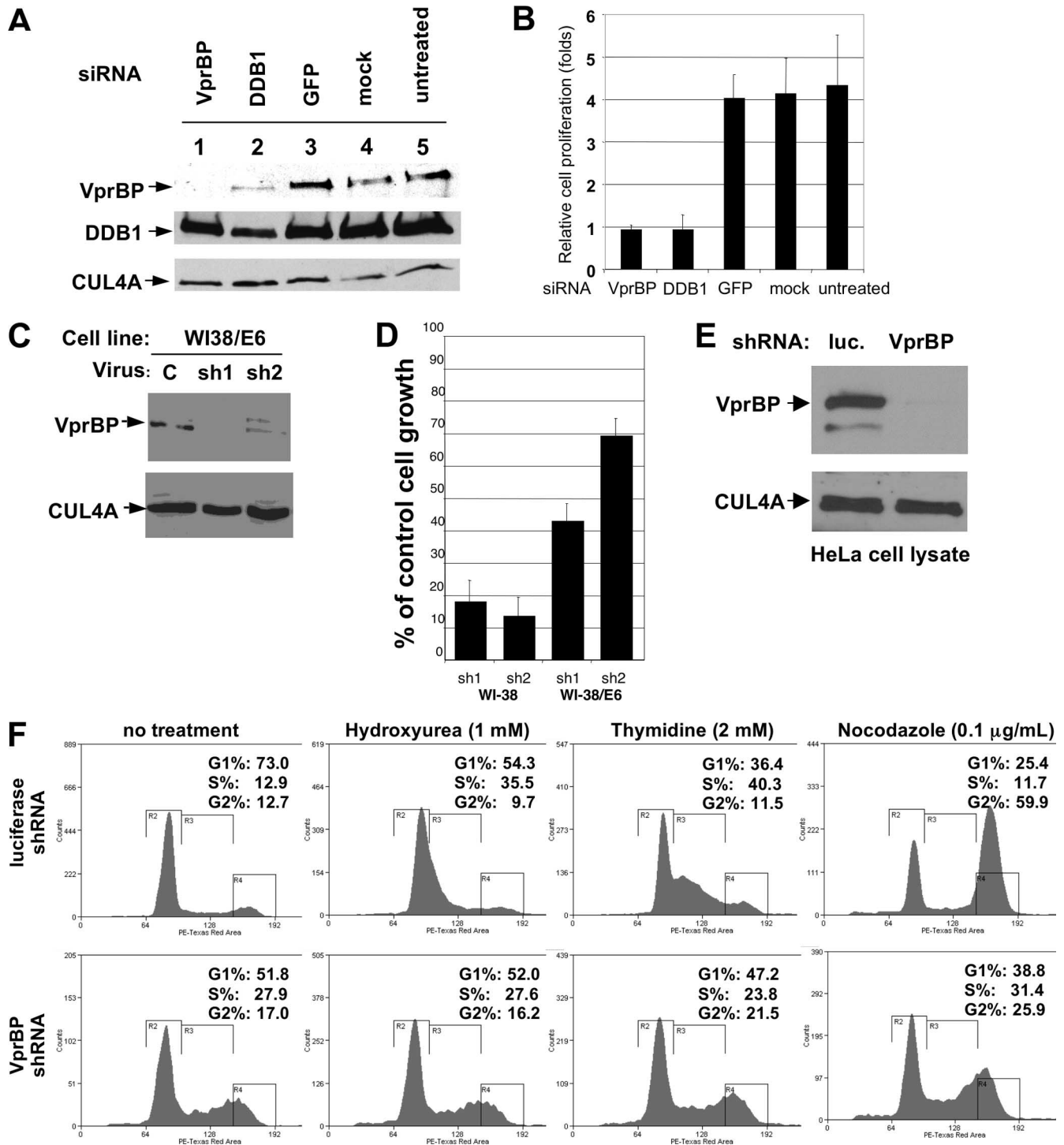
FIG. 3. VprBP is required for normal cellular proliferation and S-phase progression. (A) Recombinant Dicer-generated VprBP siRNA is efficient in silencing. U2OS cells were transfected with recombinant Dicer-generated VprBP siRNA or green fluorescent protein siRNA or synthetic DDB1 siRNA; 72 h after transfection, cells were lysed, and lysates were resolved by SDS-PAGE and immunoblotted as indicated. (B) Silencing VprBP and DDB1 inhibits cellular proliferation. At 72 h after transfection as described in panel A, equal numbers of siRNA-transfected U2OS cells were plated. The numbers of cells were counted after 72 more hours of culturing and divided by the numbers of cells initially plated, with a standard error of more than four separate counts indicated. (C) Two VprBP shRNA constructs efficiently silence expression. WI-38/E6 cells were infected with retroviruses expressing empty pMKO.1 vector (C) or vectors expressing two different shRNA sequences to VprBP (sh1 and sh2). At 24 h after infection, the cells were selected with 2 mg/ml puromycin for 48 h, and then viable cells were lysed in 0.5% NP-40 lysis buffer. Lysates were resolved by SDS-PAGE and immunoblotted as indicated. (D) Both VprBP shRNAs contribute to an inhibition of cellular proliferation. At 72 h after infection with shRNA against VprBP or empty viral vector (48 h after selection), equal numbers of viable WI-38 or WI-38/E6 cells were replated. At 72 h after plating, cell numbers were counted and normalized against empty vector control cells (control cell growth equals 100% on the graph). A standard error of more than four counts is indicated. (E) shRNA retroviruses to VprBP efficiently silence
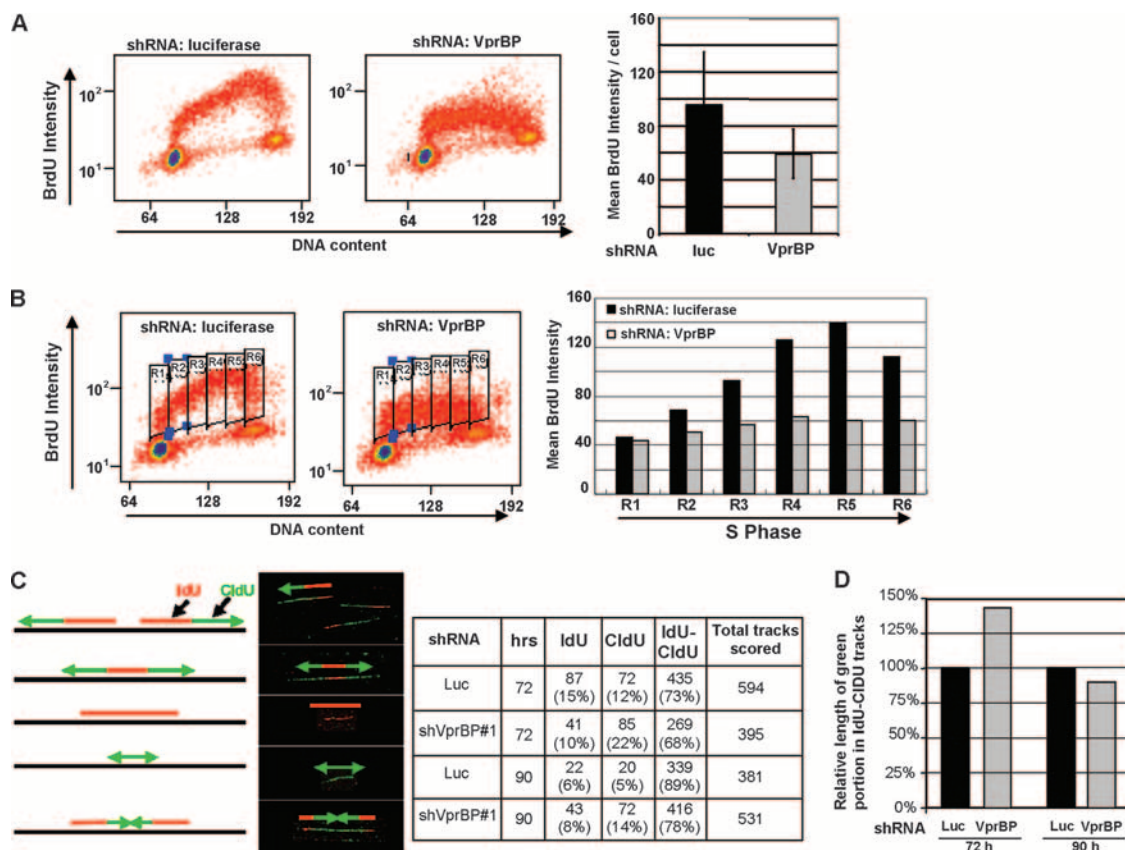
FIG. 4. VprBP silencing increases the firing of new replication forks and impairs DNA replication. (A) HeLa cells were infected with pMKO.1 retroviruses encoding shRNA to VprBP or luciferase. At 80 h postinfection, cells were selected for 56 h with puromycin (2 μg/ml) to remove uninfectecd cells and were pulse-labeled with 10 μM BrdU for 30 min. After labeling, the cells were washed with 1× PBS, trypsinized, and fixed in 80% ethanol–20% 1× PBS overnight. After cells were stained with an FITC-conjugated anti-BrdU antibody and PI, they were analyzed by flow cytometry as shown. Mean BrdU staining intensity was calculated after gating for BrdU-positive cells and graphed ± standard deviation. (B) VprBP silencing obstructs elongation of DNA replication. S-phase cells from panel A were gated into six different populations based on their DNA content, and mean BrdU intensity was calculated. (C) VprBP silencing increases newly fired origins of replication. At 72 or 90 h postinfection with shRNA retroviruses targeting either control luciferase or VprBP, HeLa cells were first labeled for 10 min with IdU, washed, and then labeled for 20 min with CldU. The cells were then trypsinized and resuspended in 1× PBS. After fixation, DNA was combed out onto the slides and stained for IdU (red) and CldU (green); individual replication tracks were counted and analyzed. After the combing step, the numbers of IdU-only, CldU-only, and IdU-CIdU tracks were quantified. (D) VprBP shRNA inconsistently affects the rate of DNA elongation. The length of green (CldU stained) sections of actively elongating (red-green) tracks were measured in HeLa cells as described in panel C, and data from control cells transduced with shRNA targeting luciferase were plotted as 100%. Luc, luciferase.

binations can be used to evaluate changes in the frequency of origin firing or replication fork progression due to an environmental stress (6, 26). As can be seen in Fig. 4C, the percentage of tracks with only the first pulse (IdU-only tracks) from two time points was similar between control cells infected with shRNA virus targeting luciferase (10%) and cells infected with shRNA virus targeting VprBP(9%), indicating that the relative number of forks that terminated during the IdU (first) pulse was unchanged by the silencing of VprBP.

However, we did find a striking change in the firing of new origins. In VprBP-silenced HeLa cells, the proportion of newly fired DNA replication forks increased significantly, i.e., from 12% and 5% in control cells infected with shRNA virus targeting luciferase to 22% and 14% in VprBP-silenced cells at 72 and 90 h after shRNA viral infection, respectively (Fig. 4C). To

VprBP expression in HeLa cells. HeLa cells were infected with pMKO.1 retroviruses encoding shRNA targeting VprBP or luciferase. At 24 h after infection, cells were selected for 48 h with 2 μg/ml puromycin. Dead cells were washed away with PBS, and selected cells were trypsinized, lysed, and analyzed for protein expression. (F) VprBP-silenced HeLa cells are arrested in S phase. Trypsinized cells from panel C were replated into new dishes. After 24 h (96 h postinfection of shRNA virus), cells were treated with hydroxyurea (1 mM), thymidine (2 mM), or nocodazole (0.1 μg/ml) as indicated. At 24 h posttreatment, cells were trypsinized and fixed overnight in 75% ethanol. After PI staining, the cell cycle was analyzed by flow cytometry. The x axes indicate PI staining intensity (DNA content); the y axes indicate cell counts. GFP, green fluorescent protein; luc, luciferase.
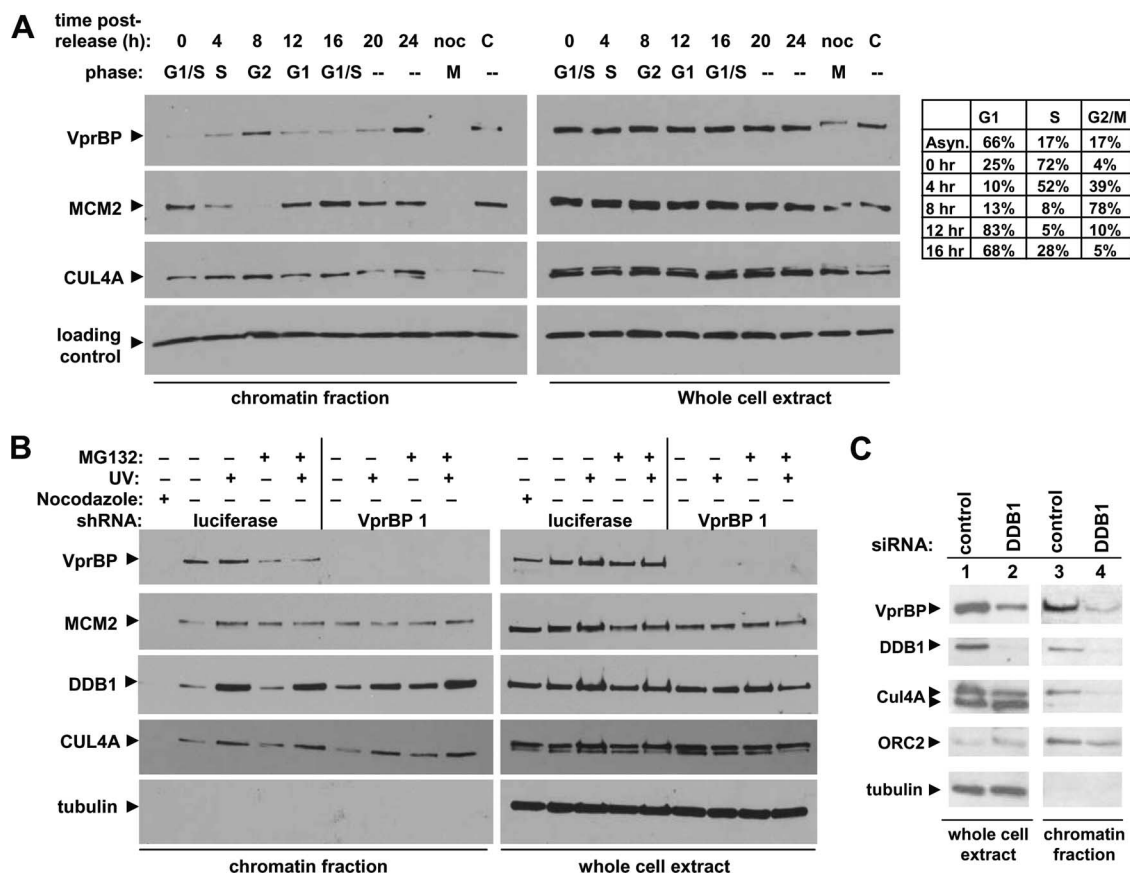
FIG. 5. VprBP and CUL4A associate with chromatin during S and G_2 phases of the cell cycle. (A) HeLa cells were synchronized at the G_1-S boundary by double-thymidine block and then released into fresh medium. Time points were collected as indicated, with a fraction of cells being fixed for flow cytometry analysis, and the rest were pelleted and frozen at $-80°C$. The frozen pellets were then chromatin fractionated (see Materials and Methods), and whole-cell extract and chromatin-associated proteins were resolved by SDS-PAGE and immunoblotted as indicated. (B) VprBP is not required for CUL4A, DDB1, or MCM2 loading onto chromatin. HeLa cells were transduced with VprBP shRNA and then selected with puromycin for 24 h starting 24 h after transduction. The cells were then passaged, and 36 h later they were trypsinized and pelleted. Pellets were fractionated as described in panel A, resolved by SDS-PAGE, and immunoblotted as indicated. Loading controls were histone H3 in the chromatin fraction and alpha-tubulin in the whole-cell extract. (C) DDB1 is not required for VprBP association with chromatin. HCT116 cells were transfected with siRNA to DDB1 or scrambled control siRNA. At 72 h posttransfection cells were collected, and chromatin fractions were prepared. When the whole-cell extract is normalized to tubulin, siRNA to the DDB1 lane resulted in 28% of the VprBP compared to the control lane. When the chromatin fraction is normalized to ORC2, siRNA to VprBP showed 42% of the VprBP, compared to the control lane, bound to chromatin.

determine whether silencing VprBP influences overall replication fork displacement rates, we measured the CldU portion of IdU-CldU (conjoined red and green) tracks in cells infected with shRNA virus targeting luciferase and VprBP. When the CldU portion of the IdU-CldU tracks was compared among the various infected cells, we could not detect any significant change in length (Fig. 4D). Therefore, we concluded that the low BrdU incorporation seen in Fig. 4B cannot be explained by the slowing down of the replication fork. One plausible explanation for the increase in the relative number of newly fired origins, combined with a decrease in BrdU incorporation, is that silencing VprBP either destabilizes replication forks or impedes the elongation of some, but not all, forks, resulting in replication stress that subsequently stimulates the firing of dormant origins (see Discussion).

VprBP associates with chromatin in a DDB1-independent and cell cycle-dependent manner. To further probe the function of VprBP in DNA replication, we determined the expres-

sion of VprBP during the cell cycle and investigated whether VprBP might directly associate with chromatin in a cell cycle-specific manner. To test this notion, we synchronized HeLa cells by arresting them at the G_1-S boundary by a double-thymidine block and then releasing them and taking samples throughout the cell cycle. We prepared either total cell lysates or fractionated lysates of these cells to enrich for chromatin-associated proteins. As the results show, the steady-state levels of VprBP remain relatively constant during interphase but decrease in nocodazole-treated cells (Fig. 5A). VprBP binds to chromatin, and the chromatin-bound fraction oscillates during the cell cycle; VprBP is not detected on chromatin in cells at the G_1-S boundary, and it increases from early S through G_2, decreases upon return to G_1 phase, and is not detectable on chromatin after arrest of cells in prometaphase by nocodazole treatment (Fig. 5B). This behavior is in contrast to MCM2, which is loaded onto chromatin to license origins in G_1 and then leaves chromatin during S phase as DNA is replicated and
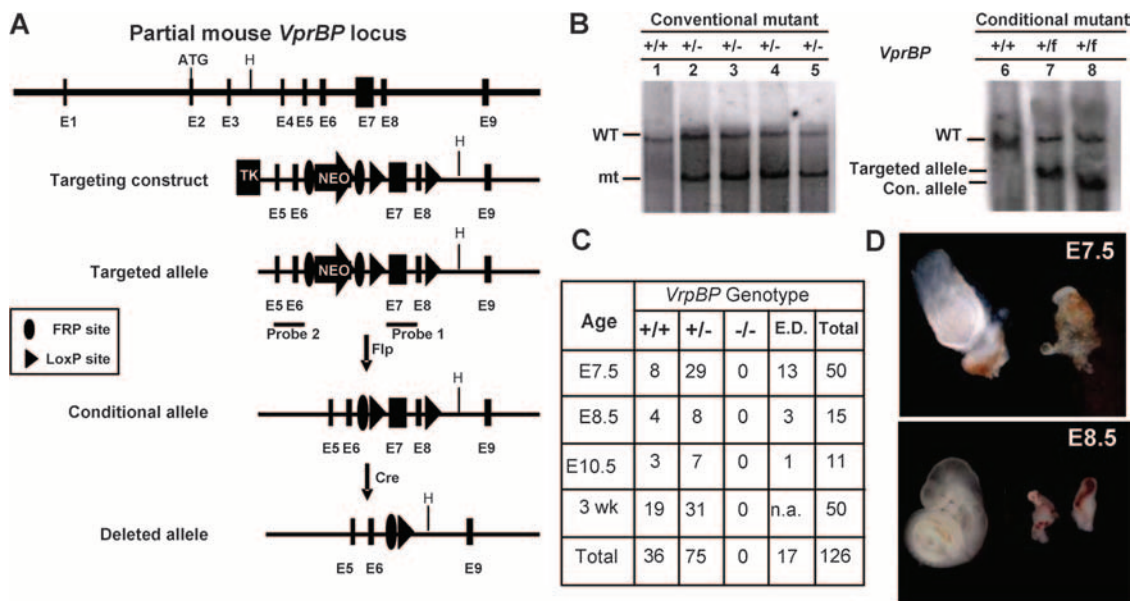
FIG. 6. *VprBP* disruption results in early embryonic lethality. (A) Disruption of the *VprBP* gene. Schematic diagram of targeting vectors and targeted alleles. (B) Southern blot analysis of genomic DNA from targeted ES clones. (Genomic DNA was digested with HindIII and probed with the internal probe (probe 2; left panel). *VprBP* ES clones displayed a 17.5-kb wild-type band and a 6.7-kb band corresponding to the knockout allele. Screening of conditional mutant clones was performed using probe 2 (right panel). The wild-type allele, the nontargeted original mutant band, and the floxed allele are indicated. (C) Embryos from *VprBP*^{+/−} heterozygous intercrosses were collected on the indicated embryonic days, and the genotypes were determined by Southern blot analysis or PCR. DNA extracted from tails of 21-day-old pups was also subjected to the same procedure. ED, empty deciduae; na, not available. (D) Morphological analysis of E7.5 and E9.5 embryos isolated from *VprBP*^{+/−} intercrosses. A typical photograph is shown for normal and mutant at E7.5 and E8.5 embryos freshly dissected from decidua. TK, thymidine kinase; WT, wild type; mt, mutant; Con, conditional.

is not detectable on chromatin in mitotic cells (40). CUL4A also binds to chromatin but exhibits a different pattern from both VprBP and MCM2: it is clearly detectable on chromatin in cells at the G_1-S boundary and remains relatively unchanged from early S to G_2. These results suggest that VprBP is recruited to chromatin as DNA is being replicated and is released from chromatin before mitosis. This interpretation is consistent with previous findings that silencing VprBP did not appreciably reduce the BrdU incorporation in cells at immediate-early S phase but caused a pronounced reduction in BrdU incorporation in cells at middle to late S phase. Moreover, silencing VprBP did not affect MCM2 chromatin loading, supporting the interpretation that VprBP functions in DNA replication at a time after formation of the prereplication complex.

The findings that VprBP strongly associates with DDB1 and binds to chromatin prompted us to explore whether VprBP may perform a function in DNA repair. We again isolated chromatin from control cells or VprBP-depleted cells that were either untreated, UV irradiated, or MG132 treated and examined chromatin association of various proteins. Consistent with a previous report (13), both DDB1 and the unneddylated form of CUL4A were associated with chromatin (Fig. 5B). No chromatin association was detected for DDB1, CUL4A, or VprBP in nocodazole-treated cells while the steady-state levels of DDB1 and CUL4A were not affected by nocodazole treatment, confirming their cell cycle-dependent association. UV treatment increased the association of DDB1 and also CUL4A with chromatin, supporting their roles in mediating the DNA damage response. In contrast to the re-

sults for DDB1 and CUL4A, UV treatment did not appreciably change either VprBP's association with chromatin or its steady-state level, suggesting that VprBP is unlikely to play a major role in a DDB1-mediated DNA damage response.

Silencing VprBP did not detectably affect CUL4A or DDB1 association with chromatin during either normal cell proliferation or after UV treatment (Fig. 5B), arguing against the model that VprBP recruits DDB1 and CUL4A to chromatin in either normal or DNA-damaged cells. Conversely, silencing DDB1 did not detectably affect VprBP binding to chromatin either (Fig. 5C). To verify this finding, we normalized the steady-state level of VprBP protein in the whole-cell extract to that of α-tubulin and the level of VprBP protein in the chromatin fraction to that of the Orc2 protein. Compared to control cells transfected with scrambled siRNA oligonucleotides, the whole-cell extract of DDB1-silenced cells contained 28% of the control amount of VprBP, whereas the chromatin fraction of DDB1-silenced cells contained 42% of control VprBP. These results suggest that chromatin binding of DDB1-CUL4 and VprBP appears to occur independently for each protein. The steady-state level of VprBP was reduced in DDB1-silenced cells as noted previously (Fig. 3A), suggesting that binding with DDB1 may stabilize VprBP.

VprBP is essential for embryonic development. To determine the in vivo function of *VprBP*, we disrupted the *VprBP* gene in murine ES cells by gene targeting (Fig. 6A and B). Two different targeting vectors were generated, one for conditional and one for conventional deletion of a 2,358-bp genomic fragment containing exons 7 and 8 encoding 203 amino acid residues (Val172 to Ala374) of mouse *VprBP* (see Materials and
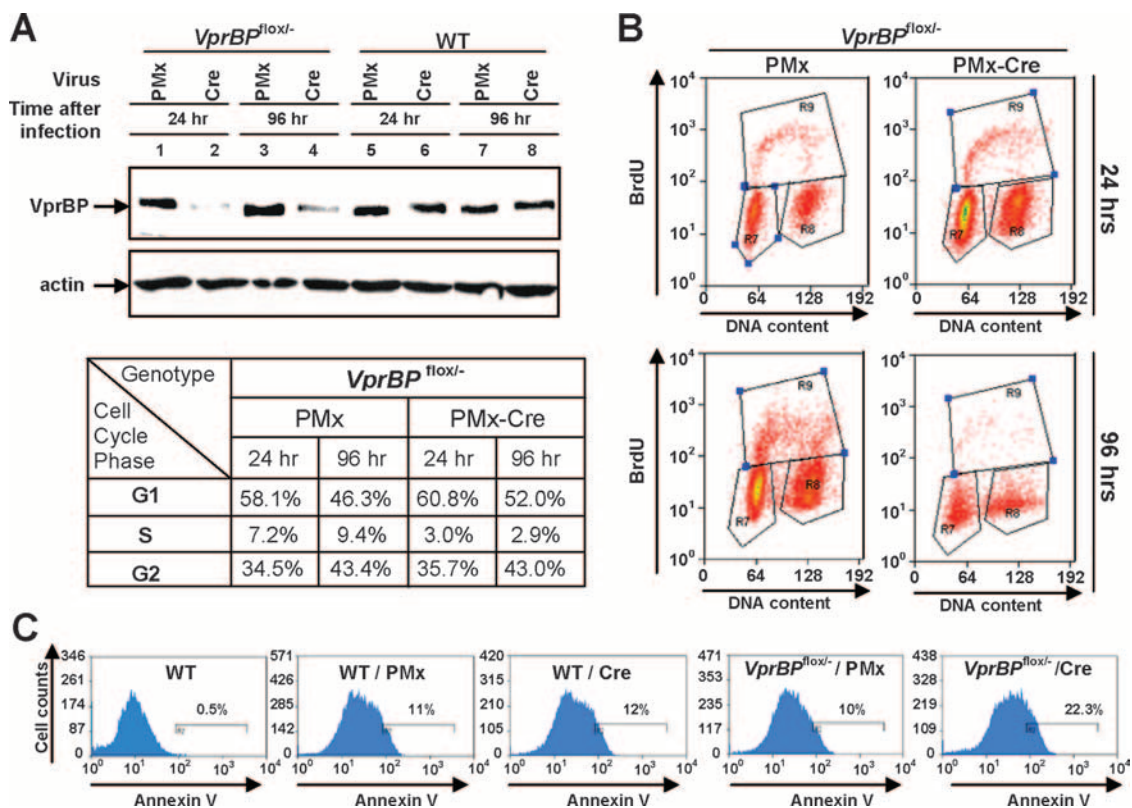
FIG. 7. *VprBP* deletion in MEFs results in reduced BrdU incorporation and increased apoptosis. (A) Wild-type (WT) and *VprBP*[flox/−] MEFs were transduced with either control pMX or pMX-Cre retroviruses. Cells were collected 24 or 96 h after puromycin selection, and *VprBP* deletion was verified by Western blotting. (B) pMX- or pMX-Cre-transduced MEFs as described in panel A were pulse-labeled with BrdU for 30 min and then fixed and stained with FITC-conjugated anti-BrdU antibody and PI. BrdU intensity and DNA content (PI intensity) were measured by flow cytometry and quantified using Summit software, version 4.3. (C) pMX- or pMX-Cre-transduced MEFs as described in panel A were selected with puromycin for 24 h and then stained with annexin V. Apoptotic cells were determined by flow cytometry.

Methods). To date, no *VprBP* null mice have been recovered, whereas *VprBP*^{+/−} and wild-type littermates were both produced at a Mendelian ratio, appeared normal, and were fertile (Fig. 6C). These data indicate that *VprBP* is essential for mouse embryonic development. To determine the time at which the *VprBP* mutation becomes lethal, we examined embryos from *VprBP*^{+/−} intercrosses at various developmental stages. All *VprBP*^{−/−} embryos between E10.5 and E13.5 were completely resorbed. Systematic analysis of embryos from day E7.5 to E9.5 generated from mating heterozygotes failed to detect *VprBP* null embryos (Fig. 6C). Empty decidua and remains of resorbed embryos were often observed at E8.5 or E7.5 in heterozygous intercrosses but were rarely seen in backcrosses between heterozygous and wild-type mice (Fig. 6D and data not shown). These results indicate that the lethality of *VprBP* null embryos may occur before E7.5.

Deletion of *VprBP* in MEFs resulted in decreased DNA replication and increased apoptosis. We also generated a conditional allele and obtained *VprBP*[flox/−] embryos at the predicted Mendelian frequencies (data not shown), confirming that the insertion of the *floxP* site into the *VprBP* locus did not cause any significant adverse effect on the function of VprBP and the development of animals. This conditional allele allowed us to derive littermate *VprBP*[flox/−] MEFs for genetically determining the function of VprBP. Infection of *VprBP*[flox/−] MEFs with a pMX-Cre retrovirus expressing the Cre recombinase resulted in nearly undetectable VprBP protein expression 24 h after infection (Fig. 7A), confirming a successful deletion of both *VprBP* alleles. At 24 and 96 h after pMX-Cre retroviral infection, we pulse-labeled wild-type and *VprBP*[flox/−] MEFs with BrdU for 1 h and examined cell cycle progression by fluorescence-activated cell sorting analysis. Twenty-four hours after pMX-Cre viral transduction, the BrdU-positive cell population was decreased by nearly 60%, from 7.2% in pMX-infected *VprBP*[flox/−] MEFs to 3.0% in pMX-Cre-infected *VprBP*[flox/−] MEFs. A substantial decrease in the S-phase cell population was also observed at a later time point, i.e., from 9.4% to 2.9% 96 h after pMX-Cre transduction (Fig. 7B). Accompanying the decrease in S-phase cell number by the deletion of *VprBP* was a small increase in the G$_1$ cell population from 58.1% to 60.8% and from 46.3% to 52% at 24 and 96 h after viral transduction, respectively. *VprBP* loss did not significantly affect the G$_2$ population. The major consequence resulting from impaired DNA replication after *VprBP* deletion is a substantial increase in apoptosis, from 10% in pMX-infected *VprBP*[flox/−] MEFs to 22.3% in pMX-Cre-infected MEFs (Fig. 7C).

DISCUSSION

In this study, we examined the cellular function of the novel DDB1-CUL4A-interacting protein VprBP, which has recently been shown to be a major target for the function of the HIV-1

Vpr protein. We demonstrated that VprBP interacts specifically with CUL4 but not other cullins and associates with the DDB1-CUL4A E3 ligase in a manner analogous to other DWD proteins, binding through DDB1 with the N terminus of CUL4A and requiring only its WD40 domain (Fig. 1 and 2). VprBP preferentially interacts with the NEDD8-modified form of CUL4A and forms a complex with the COP9/signalosome, both indicative of an active CUL4-ROC1 ligase. Together, these results suggest that VprBP functions by either recruiting specific substrates or promoting the recruitment of other substrates to the DDB1-CUL4-ROC1 E3 ligase.

Our biochemical and genetic analyses support the notion that the major functions of VprBP are mediated by DDB1. First, very little monomeric VprBP is present in the cell, and all detectable VprBP is present in fractions that are larger than 500 kDa and also contain both DDB1 and CUL4A. Second, in U2OS cells where we examined the VprBP immunocomplex by Coomassie blue staining, VprBP associates with DDB1 nearly stoichiometrically (Fig. 1). Third, genetically, deletion of the *Ddb1* gene, like that of *VprBP*, also caused early embryonic lethality, inhibition of cell proliferation, and significant apoptosis (4, 5). Although not distinct, these phenotypes are consistent with the expectation that DDB1 is essential for the function of VprBP. A direct genetic test of the functional dependency of VprBP on DDB1 is hindered by the early embryonic lethality of both *Ddb1* and *VprBP* deletions and is further complicated by the broad function of DDB1 because of its binding with as many as 90 DWD proteins.

VprBP is required for normal progression of DNA replication. The major findings of this study are that VprBP's function is essential for cells to progress through S phase and, thus, cell proliferation and embryonic development. Silencing VprBP in U2OS or WI-38 cell lines (data not shown) or deletion of the *VprBP* gene in MEFs resulted in a substantial decrease of BrdU incorporation and subsequent inhibition of cell proliferation. Silencing VprBP had no significant effect on either the binding of MCM2 to chromatin or on the BrdU incorporation in immediate-early S-phase cells, arguing against an essential function of VprBP in the assembly of the prereplication complex or in the initiation of DNA replication. Our combing experiments also indicate that termination of DNA replication appears to be normal in VprBP-depleted cells. We observed a difference in the cell cycle profile due to loss of VprBP in MEFs and HeLa cells that may be attributable to the intact p53 checkpoint pathway in MEFs. In HeLa cells, the most noticeable defect in DNA replication caused by the loss of function of VprBP is the substantial reduction of BrdU incorporation during middle to late S phase of the cell cycle and an increase in newly fired DNA replication origins (Fig. 4). These findings provide a molecular basis—controlling the progression of DNA replication—for the essential function of VprBP for cell proliferation and embryo development.

VprBP shares some notable phenotypic similarities with the *Chk1* gene. In mice, the function of both *VprBP* and *Chk1* genes are essential for MEF or ES cell viability and for early embryonic development, with *VprBP* and *Chk1* null embryos dying before E7.5 and between E3.5 and E6.5, respectively (Fig. 6) (24, 40). Codeletion of *p53* did not significantly rescue lethality of either *VprBP* (our unpublished observation) or *Chk1* null embryos (24). Both VprBP and Chk1 proteins bind

to chromatin in unperturbed cells (Fig. 5) (37), but neither plays a major function in the assembly of prereplication complexes or entry into the S phase. Instead, knocking down Chk1 or VprBP in otherwise unperturbed HeLa cells reduced the rates of replication fork progression (28) and the rate of BrdU incorporation (Fig. 4). As for Chk1-compromised cells (25), HeLa cells after the silencing of VprBP also displayed increased new origin firing (Fig. 4). We thus far have not detected any role in DNA damage checkpoints for VprBP, unlike Chk1, which is dissociated from chromatin and causes G_2/M cell cycle arrest following DNA damage. In UV-irradiated cells, we did not detect any change of either the steady-state level of VprBP or its chromatin association, nor did we detect any effects of the silencing of VprBP on the increased chromatin binding of DDB1 and CUL4A (Fig. 5B) or on CDT1 degradation (our unpublished observation). Together, these results indicate that VprBP is unlikely to play a major role in DNA repair. While the detailed biochemical mechanism underlying the function of VprBP in DNA replication is yet to be determined, we favor a model whereby VprBP functions, in a manner similar to Chk1, in the progression of DNA replication during S phase, perhaps by either maintaining the stability of forks or coordinating sequential firing of early and later origins during an unperturbed S phase, as opposed to a function of VprBP in suppressing dormant replication origins.

How does Vpr bind to VprBP to benefit HIV viral replication? Although not essential for HIV-1 replication in cell culture, the Vpr accessory protein has an important function in lentivirus pathogenesis, as evidenced by its conservation in HIV-1, HIV-2, and simian immunodeficiency virus and by the attenuated progression of AIDS in rhesus monkeys infected with simian immunodeficiency virus lacking Vpr and the very similar accessory protein Vpx (12). How Vpr facilitates HIV pathogenesis, however, remains unclear. Two consistent effects on host cells upon ectopic expression of Vpr are its ability to cause G_2 cell cycle arrest (20, 33) and its ability to activate the ATR-mediated DNA damage checkpoint pathway (34). Recently, a number of studies concurrently reported that VprBP is a major cellular binding partner of and is required for the G_2 arrest caused by Vpr (3, 8, 17, 24, 35, 39, 42). Almost all of the studies concluded that VprBP is required for Vpr-induced G_2 cell cycle arrest based on the observation that Vpr ectopic expression did not cause a G_2 accumulation in cells with VprBP knocked down. Our findings that the function of VprBP is essential for progression through S phase suggest that this conclusion needs to be viewed more cautiously. In VprBP-silenced cells, we have found that nocodazole treatment did not cause any appreciable G_2 accumulation.

Our findings favor a model that Vpr, through its interaction with VprBP, diverts the cellular chromosome replication machinery to facilitate viral replication. A consequence of this diversion by Vpr, as observed with either knocking down or deleting *VprBP*, would be reduced DNA replication and increased firing of replication origins. Two lines of evidence support this model. First, both VprBP (Fig. 5) and Vpr (23) associate with chromatin, suggesting the possibility that Vpr interacts with a chromatin-binding pool of VprBP. Second, we have shown that the function of VprBP is essential for the progression of DNA replication but not replication initiation. This finding would suggest that Vpr is more likely to interact

with VprBP to divert an ongoing chromosomal replication activity toward viral replication rather than inducing G_0 quiescent cells to enter the cell cycle. The challenging issue remains to determine whether Vpr achieves this function by increasing the activity of VprBP-DDB1-CUL4-ROC1 E3 ligase activity toward its normal substrate(s) or by hijacking the ligase to target a different substrate(s).

ACKNOWLEDGMENTS

REFERENCES

1. **Angers, S., T. Li, X. Yi, M. J. MacCoss, R. T. Moon, and N. Zheng.** 2006. Molecular architecture and assembly of the DDB1-CUL4A ubiquitin ligase machinery. Nature **443:**590–593.
2. **Bai, C., P. Sen, K. Hofmann, L. Ma, M. Goebl, J. W. Harper, and S. J. Elledge.** 1996. SKP1 connects cell cycle regulators to the ubiquitin proteolysis machinery through a novel motif, the F-box. Cell **86:**263–274.
3. **Belzile, J. P., G. Duisit, N. Rougeau, J. Mercier, A. Finzi, and E. A. Cohen.** 2007. HIV-1 Vpr-mediated G2 arrest involves the DDB1-CUL4A(VPRBP) E3 ubiquitin ligase. PLoS Pathog. **3:**e85.
4. **Cang, Y., J. Zhang, S. A. Nicholas, J. Bastien, B. Li, P. Zhou, and S. P. Goff.** 2006. Deletion of DDB1 in mouse brain and lens leads to p53-dependent elimination of proliferating cells. Cell **127:**929–940.
5. **Cang, Y., J. Zhang, S. A. Nicholas, A. L. Kim, P. Zhou, and S. P. Goff.** 2007. DDB1 is essential for genomic stability in developing epidermis. Proc. Natl. Acad. Sci. USA **104:**2733–2737.
6. **Chastain, P. D., II, T. P. Heffernan, K. R. Nevis, L. Lin, W. K. Kaufmann, D. G. Kaufman, and M. Cordeiro-Stone.** 2006. Checkpoint regulation of replication dynamics in UV-irradiated human cells. Cell Cycle **5:**2160–2167.
7. **Cook, J. G., D. A. Chasse, and J. R. Nevins.** 2004. The regulated association of Cdt1 with minichromosome maintenance proteins and Cdc6 in mammalian cells. J. Biol. Chem. **279:**9625–9633.
8. **DeHart, J. L., E. S. Zimmerman, O. Ardon, C. M. Monteiro-Filho, E. R. Arganaraz, and V. Planelles.** 2007. HIV-1 Vpr activates the G2 checkpoint through manipulation of the ubiquitin proteasome system. Virol. J. **4:**57.
9. **Feldman, R. M. R., C. C. Correll, K. B. Kaplan, and R. J. Deshaies.** 1997. A complex of Cdc4p, Skp1p, and Cdc53p/Cullin catalyzes ubiquitination of the phosphorylated CDK inhibitor Sic1p. Cell **91:**221–230.
10. **Furukawa, M., Y. J. He, C. Borchers, and Y. Xiong.** 2003. Targeting of protein ubiquitination by BTB-Cullin 3-Roc1 ubiquitin ligases. Nat. Cell Biol. **5:**1001–11007.
11. **Geyer, R., S. Wee, S. Anderson, J. Yates, and D. A. Wolf.** 2003. BTB/POZ domain proteins are putative substrate adaptors for cullin 3 ubiquitin ligases. Mol. Cell **12:**783–790.
12. **Gibbs, J. S., A. A. Lackner, S. M. Lang, M. A. Simon, P. K. Sehgal, M. D. Daniel, and R. C. Desrosiers.** 1995. Progression to AIDS in the absence of a gene for *vpr* or *vpx*. J. Virol. **69:**2378–2383.
13. **Groisman, R., J. Polanowska, I. Kuraoka, J. Sawada, M. Saijo, R. Drapkin, A. F. Kisselev, K. Tanaka, and Y. Nakatani.** 2003. The ubiquitin ligase activity in the DDB2 and CSA complexes is differentially regulated by the COP9 signalosome in response to DNA damage. Cell **113:**357–367.
14. **He, Y. J., C. M. McCall, J. Hu, Y. Zeng, and Y. Xiong.** 2006. DDB1 functions as a linker to recruit receptor WD40 proteins to CUL4-ROC1 ubiquitin ligases. Genes Dev. **20:**2949–2954.
15. **Hershko, A., and A. Ciechanover.** 1998. The ubiquitin system. Annu. Rev. Biochem. **67:**425–479.
16. **Higa, L. A., M. Wu, T. Ye, R. Kobayashi, H. Sun, and H. Zhang.** 2006. CUL4-DDB1 ubiquitin ligase interacts with multiple WD40-repeat proteins and regulates histone methylation. Nat. Cell Biol. **8:**1277–1283.
17. **Hrecka, K., M. Gierszewska, S. Srivastava, L. Kozaczkiewicz, S. K. Swanson, L. Florens, M. P. Washburn, and J. Skowronski.** 2007. Lentiviral Vpr usurps Cul4-DDB1[VprBP] E3 ubiquitin ligase to modulate cell cycle. Proc. Natl. Acad. Sci. USA **104:**11778–11783.
18. **Hu, J., C. M. McCall, T. Ohta, and Y. Xiong.** 2004. Targeted ubiquitination of CDT1 by the DDB1-CUL4A-ROC1 ligase in response to DNA damage. Nat. Cell Biol. **6:**1003–1009.
19. **Jin, J., E. E. Arias, J. Chen, J. W. Harper, and J. C. Walter.** 2006. A family of diverse Cul4-Ddb1-interacting proteins includes Cdt2, which is required for S phase destruction of the replication factor Cdt1. Mol. Cell **23:**709–721.
20. **Jowett, J. B., V. Planelles, B. Poon, N. P. Shah, M. L. Chen, and I. S. Chen.** 1995. The human immunodeficiency virus type 1 *vpr* gene arrests infected T cells in the G_2 + M phase of the cell cycle. J. Virol. **69:**6304–6313.
21. **Kamura, T., D. Burian, Q. Yan, S. L. Schmidt, W. S. Lane, E. Querido, P. E. Branton, A. Shilatifard, R. C. Conaway, and J. W. Conaway.** 2001. Muf1, a novel elongin BC-interacting leucine-rich repeat protein that can assemble with Cul5 and Rbx1 to reconstitute a ubiquitin ligase. J. Biol. Chem. **276:**29748–29753.
22. **Kamura, T., K. Maenaka, S. Kotoshiba, M. Matsumoto, D. Kohda, R. C. Conaway, J. W. Conaway, and K. I. Nakayama.** 2004. VHL-box and SOCS-box domains determine binding specificity for Cul2-Rbx1 and Cul5-Rbx2 modules of ubiquitin ligases. Genes Dev. **18:**3055–3065.
23. **Lai, M., E. S. Zimmerman, V. Planelles, and J. Chen.** 2005. Activation of the ATR pathway by human immunodeficiency virus type 1 Vpr involves its direct binding to chromatin in vivo. J. Virol. **79:**15443–15451.
24. **Le Rouzic, E., N. Belaidouni, E. Estrabaud, M. Morel, J. C. Rain, C. Transy, and F. Margottin-Goguet.** 2007. HIV1 Vpr arrests the cell cycle by recruiting DCAF1/VprBP, a receptor of the Cul4-DDB1 ubiquitin ligase. Cell Cycle **6:**182–188.
25. **Maya-Mendoza, A., E. Petermann, D. A. Gillespie, K. W. Caldecott, and D. A. Jackson.** 2007. Chk1 regulates the density of active replication origins during the vertebrate S phase. EMBO J. **26:**2719–2731.
26. **Merrick, C. J., D. Jackson, and J. F. Diffley.** 2004. Visualization of altered replication dynamics after DNA damage in human cells. J. Biol. Chem. **279:**20067–20075.
27. **Myers, J. W., J. T. Jones, T. Meyer, and J. E. Ferrell, Jr.** 2003. Recombinant Dicer efficiently converts large dsRNAs into siRNAs suitable for gene silencing. Nat. Biotechnol. **21:**324–328.
28. **Petermann, E., A. Maya-Mendoza, G. Zachos, D. A. Gillespie, D. A. Jackson, and K. W. Caldecott.** 2006. Chk1 requirement for high global rates of replication fork progression during normal vertebrate S phase. Mol. Cell. Biol. **26:**3319–3326.
29. **Petroski, M. D., and R. J. Deshaies.** 2005. Function and regulation of cullin-RING ubiquitin ligases. Nat. Rev. Mol. Cell Biol. **6:**9–20.
30. **Pick, E., O. S. Lau, T. Tsuge, S. Menon, Y. Tong, T. Dohmae, S. M. Plafker, X. W. Deng, and N. Wei.** 2007. Mammalian DET1 regulates Cul4A activity and forms stable complexes with E2 ubiquitin-conjugating enzymes. Mol. Cell. Biol. **27:**4708–4719.
31. **Pickart, C. M.** 2001. Mechanisms underlying ubiquitination. Annu. Rev. Biochem. **70:**503–533.
32. **Pintard, L., J. H. Willis, A. Willems, J. L. Johnson, M. Srayko, T. Kurz, S. Glaser, P. E. Mains, M. Tyers, B. Bowerman, and M. Peter.** 2003. The BTB protein MEL-26 is a substrate-specific adaptor of the CUL-3 ubiquitin-ligase. Nature **425:**311–316.
33. **Rogel, M. E., L. I. Wu, and M. Emerman.** 1995. The human immunodeficiency virus type 1 *vpr* gene prevents cell proliferation during chronic infection. J. Virol. **69:**882–888.
34. **Roshal, M., B. Kim, Y. Zhu, P. Nghiem, and V. Planelles.** 2003. Activation of the ATR-mediated DNA damage response by the HIV-1 viral protein R. J. Biol. Chem. **278:**25879–25886.
35. **Schrofelbauer, B., Y. Hakata, and N. R. Landau.** 2007. HIV-1 Vpr function is mediated by interaction with the damage-specific DNA-binding protein DDB1. Proc. Natl. Acad. Sci. USA **104:**4130–4135.
36. **Skowyra, D., K. Craig, M. Tyers, S. J. Elledge, and J. W. Harper.** 1997. F-box proteins are receptors that recruit phosphorylated substrates to the SCF ubiquitin-ligase complex. Cell **91:**209–219.
37. **Smits, V. A., P. M. Reaper, and S. P. Jackson.** 2006. Rapid PIKK-dependent release of Chk1 from chromatin promotes the DNA-damage checkpoint response. Curr. Biol. **16:**150–159.
38. **Stebbins, C. E., W. G. Kaelin, Jr., and N. P. Pavletich.** 1999. Structure of the VHL-ElonginC-ElonginB complex: implications for VHL tumor suppressor function. Science **284:**455–461.
39. **Tan, L., E. Ehrlich, and X. F. Yu.** 2007. DDB1 and Cul4A are required for HIV-1 Vpr-induced G_2 arrest. J. Virol. **81:**10822–10830.
40. **Tanaka, T., D. Knapp, and K. Nasmyth.** 1997. Loading of an Mcm protein onto DNA replication origins is regulated by Cdc6p and CDKs. Cell **90:**649–660.
41. **Unsal-Kacmaz, K., P. D. Chastain, P. P. Qu, P. Minoo, M. Cordeiro-Stone, A. Sancar, and W. K. Kaufmann.** 2007. The human Tim/Tipin complex coordinates an intra-S checkpoint response to UV that slows replication fork displacement. Mol. Cell. Biol. **27:**3131–3142.
42. **Wen, X., K. M. Duus, T. D. Friedrich, and C. M. de Noronha.** 2007. The HIV1 protein VPR acts to promote G2 cell cycle arrest by engaging a DDB1 and cullin4A containing ubiquitin ligase complex using VPRBP/DCAF1 as an adaptor. J. Biol. Chem. **282:**27046–27057.
43. **Xu, L., Y. Wei, J. Reboul, P. Vaglio, T. H. Shin, M. Vidal, S. J. Elledge,**

and J. W. Harper. 2003. BTB proteins are substrate-specific adaptors in an SCF-like modular ubiquitin ligase containing CUL-3. Nature **425:**316–321.

44. **Zhang, J. G., A. Farley, S. E. Nicholson, T. A. Willson, L. M. Zugaro, R. J. Simpson, R. L. Moritz, D. Cary, R. Richardson, G. Hausmann, B. J. Kile, S. B. Kent, W. S. Alexander, D. Metcalf, D. J. Hilton, N. A. Nicola, and M.**

Baca. 1999. The conserved SOCS box motif in suppressors of cytokine signaling binds to elongins B and C and may couple bound proteins to proteasomal degradation. Proc. Natl. Acad. Sci. USA **96:**2071–2076.

45. **Zhang, S., Y. Feng, O. Narayan, and L. J. Zhao.** 2001. Cytoplasmic retention of HIV-1 regulatory protein Vpr by protein-protein interaction with a novel human cytoplasmic protein VprBP. Gene **263:**131–140.